

Chimera states and the interplay between initial conditions and non-local coupling

Peter Kalle,¹ Jakub Sawicki,¹ Anna Zakharova,¹ and Eckehard Schöll¹

Institut für Theoretische Physik, Technische Universität Berlin, Hardenbergstraße 36, 10623 Berlin, Germany

(Dated: 1 June 2022)

Chimera states are complex spatio-temporal patterns that consist of coexisting domains of coherent and incoherent dynamics. We study chimera states in a network of non-locally coupled Stuart-Landau oscillators. We investigate the impact of initial conditions in combination with non-local coupling. Based on an analytical argument, we show how the coupling phase and the coupling strength are linked to the occurrence of chimera states, flipped profiles of the mean phase velocity, and the transition from a phase- to an amplitude-mediated chimera state.

PACS numbers: 05.45.Xt, 87.18.Sn, 89.75.-k

Keywords: nonlinear systems, dynamical networks, coherence, chimeras, spatial chaos

Chimera states are an example of intriguing partial synchronization patterns appearing in networks of identical oscillators with symmetric coupling scheme. They exhibit a hybrid structure combining coexisting spatial domains of coherent (synchronized) and incoherent (desynchronized) dynamics, and were first reported for the model of phase oscillators^{1,2}. Recent studies have demonstrated the emergence of chimera states in a variety of topologies, and for different types of individual dynamics^{3,4}. In this paper, the interplay between initial conditions and non-local coupling is studied. We show that, based on an analytical argument incorporating the initial conditions and the range of non-local coupling, the occurrence of phase chimeras can be seen as caused by a phase lag in the coupling. Considering the dynamics of chimera states, our argument shows how “flipped” profiles of the mean phase velocities can be explained by a change of sign of the coupling phase. By this, one can either choose a concave (“upside”) profile of the mean phase velocities, or a “flipped” one. Extending our reasoning, we show that this argument intuitively explains the transition from phase- to amplitude-mediated chimera state as a result of increasing coupling strength.

cluding time-discrete maps^{8–10}, time-continuous chaotic models¹¹, neural systems^{12–15}, Boolean networks¹⁶, population dynamics^{17,18}, Van der Pol oscillators^{19,20}, and quantum oscillator systems²¹. Moreover, chimera states allow for higher spatial dimensions^{3,22–24}. Together with the initially reported chimera states, which consist of one coherent and one incoherent domain, new types of these peculiar states having multiple^{12,19,25–27} or alternating²⁸ incoherent regions, as well as amplitude-mediated^{29,30}, and pure amplitude chimera and chimera death states^{31,32} were discovered. A classification has recently been given³³. In many systems, the form of the coupling defines the possibility to obtain chimera states. The nonlocal coupling has generally been assumed to be a necessary condition for chimera states to evolve in coupled systems. However, recent studies have shown that even global all-to-all coupling^{30,34–37}, as well as more complex coupling topologies allow for the existence of chimera states^{14,15,17,20,38}. Furthermore, time-varying network structures can give rise to alternating chimera states³⁹. Chimera states have also been shown to be robust against inhomogeneities of the local dynamics and coupling topology^{14,40}, as well as against noise⁴¹, or they might even be induced by noise^{42,43}. Possible applications of chimera states in natural and technological systems include the phenomenon of uni-hemispheric sleep^{44,45}, bump states in neural systems^{46,47}, epileptic seizures⁴⁸, power grids⁴⁹, or social systems⁵⁰. Many works considering chimera states have mostly been based on numerical results. A deeper bifurcation analysis⁵¹ and even a possibility to control chimera states^{52–54} were obtained only recently. The experimental verification of chimera states was first demonstrated in optical⁵⁵ and chemical^{56,57} systems. Further experiments involved mechanical^{58,59}, electronic^{60,61}, optoelectronic delayed-feedback⁶² and electrochemical^{63,64} oscillator systems, Boolean networks¹⁶, and optical combs⁶⁵.

I. INTRODUCTION

The analysis of coupled oscillatory systems is an important research field bridging between nonlinear dynamics, network science, and statistical physics, with a variety of applications in physics, biology, and technology^{5,6}. The last decade has seen an increasing interest in chimera states in dynamical networks^{3,4,7}. First obtained in systems of phase oscillators^{1,2}, chimeras can also be found in a large variety of different systems in-

Motivated by these studies, the goal of the present manuscript is to discuss how a specific set of initial conditions initially separating the network into distinct do-

mains gives rise to a clustered chimera state. This approach allows three statements to be validated: First, it will be discussed how this approach provides an intuitive answer to the question why a pronounced off-diagonal coupling (a coupling phase α close to $\pi/2$) is needed in order to access chimera states. Second, it will be explained how a change of the sign of the coupling phase α leads to the occurrence of normal and “flipped” arch-shaped profiles of the mean phase velocities, respectively. These profiles are believed to be a distinct feature of (phase) chimeras, at least in the case of non-locally coupled systems. Third, it will be discussed how an increase of the coupling strength σ is linked to a transition from a pure phase chimera state to a coupled phase-amplitude chimera state. The latter shows the main properties of an amplitude-mediated chimera state²⁹, i.e., the variations in the phases are connected with non-vanishing variations in the amplitudes.

II. MODEL

We consider a ring network of non-locally coupled Stuart-Landau oscillators. The local dynamics is given by the generic expansion (normal form) of an oscillator near a supercritical Hopf bifurcation

$$\dot{z} = (\lambda + i\omega)z - |z|^2 z, \quad (1)$$

where $\lambda \in \mathbb{R}$ is the bifurcation parameter, $\omega > 0$ is the frequency of the self-sustained oscillation and $z \in \mathbb{C}$ is the dynamical variable. In the co-rotating frame⁶⁶, applying an appropriate scaling of time t , space x , and z ,

$$\tilde{t} = \lambda t, \quad (2)$$

$$\tilde{x} = \lambda^{-1} x, \quad (3)$$

$$\tilde{z} = \lambda^{-1/2} \exp(-i\omega t) z, \quad (4)$$

and then dropping the tilde, the local dynamics is simplified to

$$\dot{z} = (1 - |z|^2)z = f(z), \quad (5)$$

where $\lambda > 0$ has been assumed. The network can be described in the continuum limit by the following partial differential equation,

$$\partial_t z(x, t) = f(z) + \sigma e^{i\alpha} \int_0^L G(x - x') [z(x') - z(x)] dx', \quad (6)$$

where the local dynamics $f(z)$ of an oscillator is given by Eq. (5), σ is the coupling strength, α is the coupling phase, L is the system size assuming periodic boundary conditions, and $G(x - x')$ is the coupling kernel determining the functional shape and range of the non-local coupling. Here we assume that the kernel is given by a Gaussian with mean zero

$$G(x - x') = c e^{-|x-x'|^2}, \quad (7)$$

where $c = 1/\Gamma(\frac{1}{2})$ denotes the normalization factor and Γ is the gamma-function, but our results hold also for more general kernels.

To motivate a specific choice of parameters and initial conditions governing the emergence of chimera states, the system is transformed to polar coordinates via $z = r \exp(i\theta)$. This yields the following partial differential equations that describe the evolution of the amplitude r and phase θ ,

$$\partial_t r(x, t) = F(r) + \underbrace{\sigma \int_0^L G(x - x') [r(x') \cos(\theta(x') - \theta(x) + \alpha) - r(x) \cos(\alpha)] dx'}_{\Sigma_r}, \quad (8)$$

$$\partial_t \theta(x, t) = \underbrace{\sigma \int_0^L G(x - x') \left[\frac{r(x')}{r(x)} \sin(\theta(x') - \theta(x) + \alpha) - \sin(\alpha) \right] dx'}_{\Sigma_\theta}. \quad (9)$$

The local dynamics of the amplitudes is given by $F(r) = (1 - r^2)r$ with a stable fixed point $r_0 = 1$. In the following we study the impact of the non-local coupling on the dynamics of the network. Introducing the amplitude coupling Σ_r and the phase coupling Σ_θ we can write Eqs. (8)

and (9) as

$$\partial_t r(x, t) = F(r) + \Sigma_r(x, t), \quad (10)$$

$$\partial_t \theta(x, t) = \Sigma_\theta(x, t). \quad (11)$$

For the numerical simulations we use the discretized

version of Eq. (6), i.e., a ring of N coupled oscillators

$$\dot{z}_j = f(z_j) + \sigma e^{i\alpha} \sum_{k=1}^N G_{jk} [z_k - z_j], \quad (12)$$

where $j = 1, \dots, N$ and all indices are modulo N . $G_{jk} = \Delta x G(\Delta x [j - k])$ is the discretized version of the coupling kernel in Eq. (7), where $\Delta x = L/N$ is the spatial increment between neighboring oscillators.

III. THE IMPACT OF INITIAL CONDITIONS

An important issue, often considered as a necessary condition for the existence of chimera states, is the choice of initial conditions. Random initial conditions do not always guarantee chimera behavior. This is due to the fact that classical chimera states typically coexist with the completely synchronized regime. In the case of chimera states the basin of attraction can be relatively small in comparison with that of the synchronized state. In the present work we discuss the impact of specially prepared initial conditions and non-local coupling in order to explain, predict and confirm the occurrence of chimera states and their main features.

A. From initial conditions to a clustered chimera state

Using an anti-phase cluster as initial condition, it is possible to simplify the initial coupling terms in amplitude and phase significantly. The initial conditions are chosen as two clusters in anti-phase,

$$r(x, t_0) = 1, \quad (13)$$

$$\theta(x, t_0) = \begin{cases} \pi & , \text{ if } x \in (0, L/2] \\ 0 & , \text{ if } x \in (L/2, L] \end{cases}. \quad (14)$$

The network is initially divided into two equally sized domains. The first one, with phase π , reaches from 0 to $L/2$. The second one, with phase 0, reaches from $L/2$ to L . By this choice of two domains in anti-phase, the network is initially spatially separated into four distinct domains with respect to the coupling terms Σ_r and Σ_θ . This is schematically shown in Fig. 1. Two domains, where the coupling terms vanish because the oscillators are coupled solely to oscillators in phase (Fig. 1a), are separated by two domains where the coupling terms Σ_r and Σ_θ have finite, non-vanishing values due to the coupling to oscillators that are in anti-phase (Fig. 1b). This initial separation influences the corresponding long-time behavior significantly. While the dynamics of the two populations with almost vanishing coupling terms becomes synchronized, the two populations where the coupling does not vanish initially, are perturbed in their phase and amplitude dynamics, see Fig. 1c. The corresponding chimera state can be clearly seen in a space-time plot, where the

dynamics is shown for the real parts $Re(z_j)$ for every node of the network (Fig. 2). The two populations of oscillators being initially in anti-phase split into the four domains mentioned. Two clusters in anti-phase are formed around the centers of the initial in-phase domains at $x = L/4$ ($j = 25$) and $x = 3L/4$ ($j = 75$). The two coherent domains are separated by incoherent domains, their initial centers being at $x = L/2$ ($j = 50$) and $x = L$ ($j = 100$).

The validity of this approach has been tested for long simulation times and increasing numbers of oscillators forming the network. Our simulations confirm that the observed chimera states are long-living and rule out finite-size effects for oscillator numbers up to $N = 1001$.

B. Off-diagonal coupling revisited

It has been shown recently that a value of the coupling phase $\alpha \simeq \pi/2$ is required for chimera states in phase oscillators^{2,12}. Also the chimera state shown in Fig. 2 requires a coupling phase α close to $\pi/2$ in order to be observed. Such a condition has been used in many studies^{2,12,52}. We show that the approach outlined in the previous section gives an intuitive explanation of this property. Furthermore, it allows us to predict and explain the occurrence of “flipped” profiles of the mean phase velocities.

To this purpose, we study the initial dynamics that is simplified by the initial conditions. The amplitude initial conditions, Eq. (13), result in vanishing local dynamics of the amplitudes, $F(r, t_0) = 0$, and the initial dynamics is simplified to

$$\partial_t r(x, t_0) = \Sigma_r(x, t_0), \quad (15)$$

$$\partial_t \theta(x, t_0) = \Sigma_\theta(x, t_0). \quad (16)$$

Using the initial conditions, Eqs. (13) and (14), in the definitions of the coupling terms given by Eqs. (8) and (9), the initial coupling terms are simplified to

$$\Sigma_r(x, t_0) = -\sigma \cos(\alpha) C_r(x), \quad (17)$$

$$\Sigma_\theta(x, t_0) = -\sigma \sin(\alpha) C_\theta(x), \quad (18)$$

where the function $C_r(x)$ summarizes the values of the integral in the amplitude dynamics and other constants, and the function $C_\theta(x)$ summarizes the values of the integral in the phase dynamics and other constants. If we now take a look at the scenario sketched in Fig. 1, the mechanism leading to a chimera state is uncovered: While the functions representing the integral vanish towards the center of the synchronized domains, leading to synchronized behavior, their non-zero values towards the borders between the anti-phase domains leads to varying, desynchronized behavior.

For α close to $\pi/2$ the amplitude coupling term $\Sigma_r(x, t_0)$ nearly vanishes and the magnitude of the phase

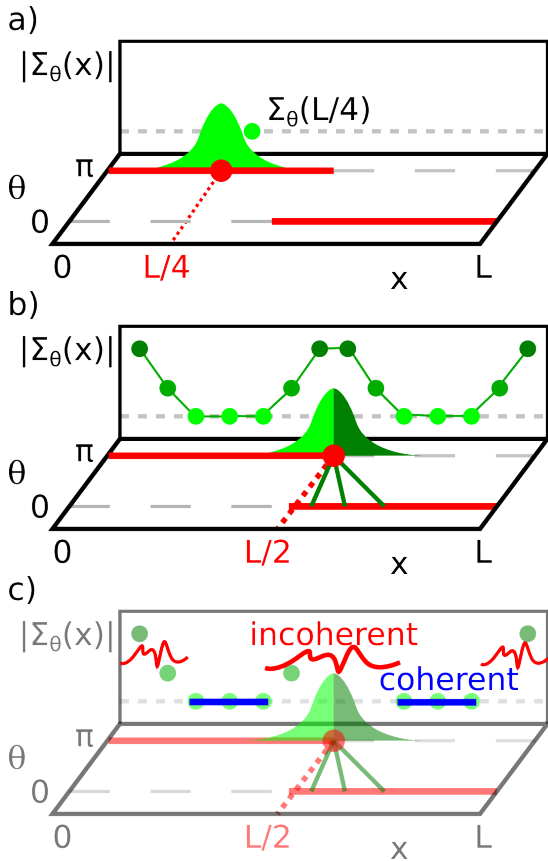


FIG. 1. Sketch of the initial dynamical scenario obtained by the choice of two populations initially in anti-phase, as given by Eq. (14). The distribution of the phases θ vs space x is shown by full red lines. The coupling kernel $G(x - x')$ localized at a specific oscillator (red dot) is shaded (green). (a) Oscillator at the center of an in-phase population at $x_0 = L/4$, yielding a vanishing coupling term $\Sigma_\theta = 0$. (b) Oscillator at the border between in-phase and anti-phase populations $x_c = L/2$, yielding a maximum coupling term $\Sigma_\theta(x_c)$. The green connected dots sketch the profile of the coupling term Σ_θ vs x . The magnitude of the initial coupling term $\Sigma_\theta(x)$ is illustrated by the brightness of the green color. There are four distinct regions, two where the coupling term nearly vanishes, and two where it does not (note the periodic boundary conditions in x). (c) Sketch of the dynamical scenario arising from this distribution of the initial coupling term. The blue straight lines illustrate coherent states with a constant phase, where the phase dynamics of the oscillators is not perturbed by the coupling term. The red twisted lines denote incoherent states with varying phases. These are centered around the borders between the two oscillator population. In these regions the coupling term does not vanish due to the non-local coupling to oscillators in anti-phase.

coupling term $\Sigma_\theta(x, t_0)$ is maximum, thus effectively restricting the variation to the phases. It is important to note that this effect of the initial coupling terms in Eqs. (17) and (18) also occurs if the coupling phase α approaches the value $-\pi/2$. This property is used in the next subsection where the occurrence of "flipped" profiles

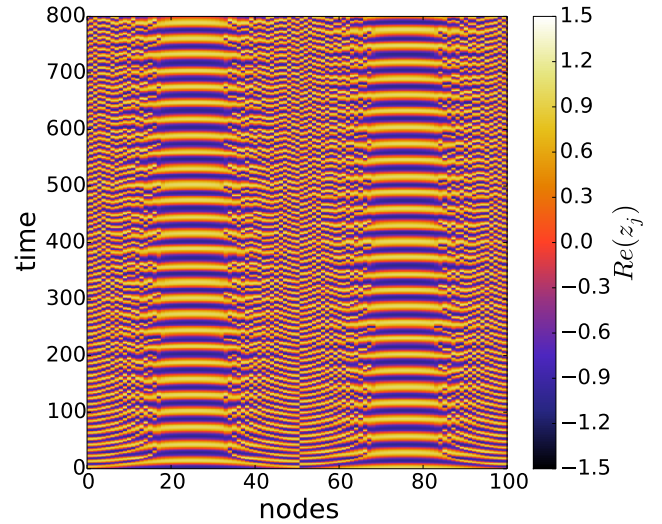


FIG. 2. Space-time plot of $Re(z_j)$ in a network of N non-locally coupled oscillators. The initial conditions are given by Eqs. (13) and (14). Parameters: $\sigma = 0.6$, $\alpha = \pi/2 - 0.15$, $N = 101$, $L = 2\pi$.

of the mean phase velocities and its connection to the coupling phase α is discussed. The possibility to increase amplitude modulations by a proper choice of coupling strength σ is analyzed in the subsequent section.

C. "Flipping" profiles of the mean phase velocities

From Eq. (16) it follows that the sign of the phases is determined by the phase coupling term $\Sigma_\theta(x, t)$ solely. Therefore, a change in the sign of Σ_θ changes the phase dynamics qualitatively. In particular, for positive values of Σ_θ the phases are expected to evolve to positive values while for negative values of Σ_θ the phases become negative. In the first case, a positive phase velocity results in a normal concave "upside" profile of the mean phase velocities $\omega_j = \partial_t \theta(x_j)$, while in the latter case negative values of the phase velocities lead to a convex "flipped" profile of the mean phase velocities, see Fig. 3.

The sign of Σ_θ is changed by a suitable choice of α . Coupling phases α close to $-\pi/2$ fulfill the requirement of almost vanishing amplitude coupling terms Σ_r and maximum magnitude of the phase coupling terms Σ_θ , as well. Taking advantage of this, the sign of the coupling terms can be modified by a change of the sign of α . As shown in Fig. 3a a value of $\alpha = \pi/2 - 0.15$ leads to a negative sign of the coupling terms Σ_θ , and a "flipped" profile of the mean phase velocities can be observed for the domains of incoherent phases. In contrast, in Fig. 3b a choice of $\alpha = -(\pi/2 - 0.15)$ results in a positive coupling term Σ_θ , leading to a normal concave "upside" profile of positive mean phase velocities.

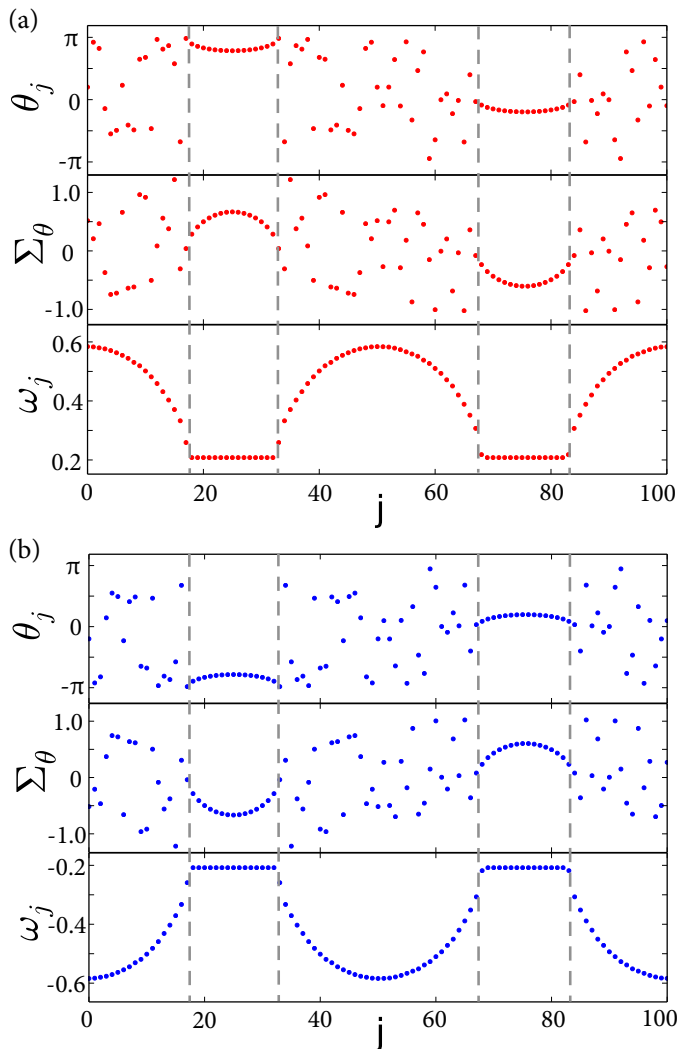


FIG. 3. Snapshots of the phases θ_j (top panels), phase coupling term Σ_θ (middle panels) and profile of the mean phase velocities ω_j (bottom panels) at $t = 400$ for (a) $\alpha = -(\pi/2 - 0.15)$ and (b) $\alpha = \pi/2 - 0.15$. Initial conditions and parameters as in Fig. 2.

D. Transition from phase to amplitude-phase chimera states

A feature of amplitude-mediated chimera states, as reported recently²⁹, is the coexistence of coherent and incoherent domains not only for the phases but also for the amplitudes. By inspecting the simplified coupling term in the amplitudes, Σ_r , it is possible to explain the transition from phase chimera states to amplitude-phase chimera states by increasing the coupling strength σ . As discussed above, the initial dynamics for the amplitudes is simplified to

$$\partial_t r(x, t_0) = \Sigma_r(x, t_0), \quad (19)$$

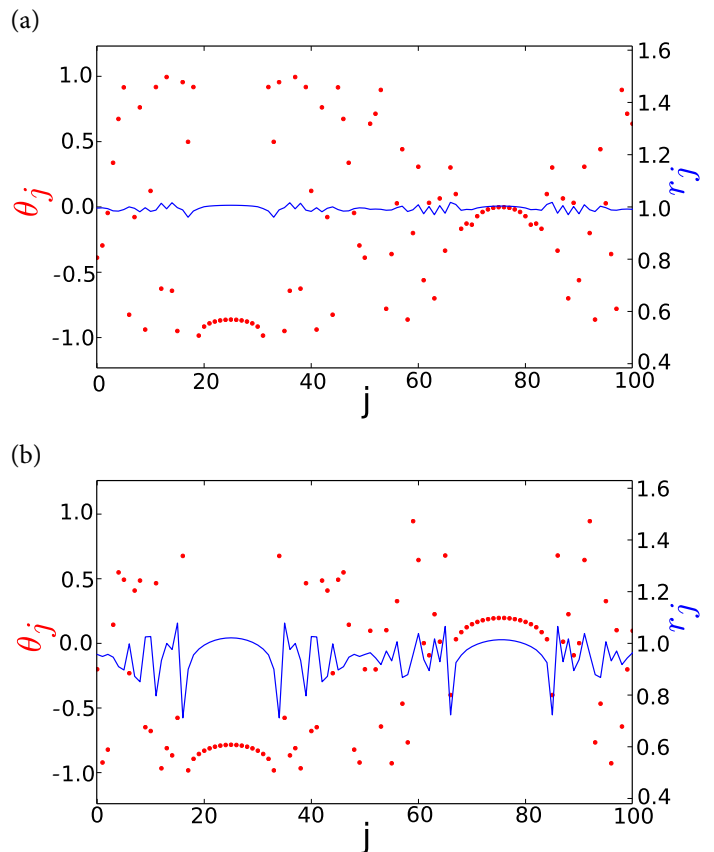


FIG. 4. Snapshots of the phase θ_j (red dots) and amplitudes r_j (blue lines) at $t = 2000$ for (a) weak coupling strength, $\sigma = 0.1$, and (b) increased coupling strength, $\sigma = 0.6$. Initial conditions and other parameters as in Fig. 2.

where the coupling term for the amplitudes is given by

$$\Sigma_r(x, t_0) = -\sigma \cos(\alpha) C_r(x). \quad (20)$$

The magnitude of the coupling term Σ_r increases linearly by the coupling strength σ . Therefore, in the limit of weak coupling ($\sigma = 0.1$) the occurrence of a phase chimera is expected, where the variations in the amplitudes are negligible, see Fig. 4a. In contrast, as shown in Fig. 4b, for increased values of the coupling strength ($\sigma = 0.6$) the amplitude variations increase and the incoherent dynamics of the phases is combined with non-vanishing modulations in the amplitudes r_j .

IV. CONCLUSION

In the current study, we have analyzed chimera states in networks of Stuart-Landau oscillators. We have provided an analytical argument that explains the need for an off-diagonal coupling, i.e., a phase-lag in the coupling, in order to create chimera states. Based on this, we have discussed the impact of the sign of the coupling

phases. We were able to show how the sign of the coupling phase determines the sign of the profile of the mean phase velocities. Furthermore, we exemplified how our argument gives an intuitive explanation for the transition from phase chimera states in the limit of weak coupling to a state sharing the main features of an amplitude-mediated chimera state in the case of intermediate coupling strength.

ACKNOWLEDGMENTS

This work was supported by Deutsche Forschungsgemeinschaft in the framework of Collaborative Research Center SFB 910.

- ¹Y. Kuramoto and D. Battogtokh, *Nonlin. Phen. in Complex Sys.* **5**, 380 (2002).
- ²D. M. Abrams and S. H. Strogatz, *Phys. Rev. Lett.* **93**, 174102 (2004).
- ³M. J. Panaggio and D. M. Abrams, *Nonlinearity* **28**, R67 (2015).
- ⁴E. Schöll, *Eur. Phys. J. Spec. Top.* **225**, 891 (2016).
- ⁵A. Pikovsky, M. G. Rosenblum, and J. Kurths, *Synchronization, A Universal Concept in Nonlinear Sciences* (Cambridge University Press, Cambridge, 2001).
- ⁶S. Boccaletti, V. Latora, Y. Moreno, M. Chavez, and D. U. Hwang, *Phys. Rep.* **424**, 175 (2006).
- ⁷C. R. Laing, *Physica D* **238**, 1569 (2009).
- ⁸I. Omelchenko, Y. Maistrenko, P. Hövel, and E. Schöll, *Phys. Rev. Lett.* **106**, 234102 (2011).
- ⁹V. Semenov, A. Feoktistov, T. Vadivasova, E. Schöll, and A. Zakharova, *Chaos* **25**, 033111 (2015).
- ¹⁰T. E. Vadivasova, G. Strelkova, S. A. Bogomolov, and V. Anishchenko, *Chaos* **26**, 093108 (2016).
- ¹¹I. Omelchenko, B. Riemenschneider, P. Hövel, Y. Maistrenko, and E. Schöll, *Phys. Rev. E* **85**, 026212 (2012).
- ¹²I. Omelchenko, O. E. Omel'chenko, P. Hövel, and E. Schöll, *Phys. Rev. Lett.* **110**, 224101 (2013).
- ¹³J. Hizanidis, V. Kanas, A. Bezerianos, and T. Bountis, *Int. J. Bifurcation Chaos* **24**, 1450030 (2014).
- ¹⁴I. Omelchenko, A. Provata, J. Hizanidis, E. Schöll, and P. Hövel, *Phys. Rev. E* **91**, 022917 (2015).
- ¹⁵N. D. Tsigkri-DeSmedt, J. Hizanidis, P. Hövel, and A. Provata, *Eur. Phys. J. Spec. Top.* **225**, 1149 (2016).
- ¹⁶D. P. Rosin, D. Rontani, and D. J. Gauthier, *Phys. Rev. E* **89**, 042907 (2014).
- ¹⁷J. Hizanidis, E. Panagakou, I. Omelchenko, E. Schöll, P. Hövel, and A. Provata, *Phys. Rev. E* **92**, 012915 (2015).
- ¹⁸T. Banerjee, P. S. Dutta, A. Zakharova, and E. Schöll, *Phys. Rev. E* **94**, 032206 (2016).
- ¹⁹I. Omelchenko, A. Zakharova, P. Hövel, J. Siebert, and E. Schöll, *Chaos* **25**, 083104 (2015).
- ²⁰S. Ulonska, I. Omelchenko, A. Zakharova, and E. Schöll, *Chaos* **26**, 094825 (2016).
- ²¹V. Bastidas, I. Omelchenko, A. Zakharova, E. Schöll, and T. Brandes, *Phys. Rev. E* **92**, 062924 (2015).
- ²²O. E. Omel'chenko, M. Wolfrum, S. Yanchuk, Y. Maistrenko, and O. Sudakov, *Phys. Rev. E* **85**, 036210 (2012).
- ²³S.-i. Shima and Y. Kuramoto, *Phys. Rev. E* **69**, 036213 (2004).
- ²⁴Y. Maistrenko, O. Sudakov, O. Osiv, and V. Maistrenko, *New J. Phys.* **17**, 073037 (2015).
- ²⁵A. Vüllings, E. Schöll, and B. Lindner, *Eur. Phys. J. B* **87**, 31 (2014).
- ²⁶G. C. Sethia, A. Sen, and F. M. Atay, *Phys. Rev. Lett.* **100**, 144102 (2008).
- ²⁷J. Xie, E. Knobloch, and H. C. Kao, *Phys. Rev. E* **90**, 022919 (2014).
- ²⁸S. W. Haugland, L. Schmidt, and K. Krischer, *Sci. Rep.* **5**, 9883 (2015).
- ²⁹G. C. Sethia, A. Sen, and G. L. Johnston, *Phys. Rev. E* **88**, 042917 (2013).
- ³⁰G. C. Sethia and A. Sen, *Phys. Rev. Lett.* **112**, 144101 (2014).
- ³¹A. Zakharova, M. Kapeller, and E. Schöll, *Phys. Rev. Lett.* **112**, 154101 (2014).
- ³²T. Banerjee, *Europhys. Lett.* **110**, 60003 (2015).
- ³³F. P. Kemeth, S. W. Haugland, L. Schmidt, I. G. Kevrekidis, and K. Krischer, *Chaos* **26**, 094815 (2016).
- ³⁴A. Yeldesbay, A. Pikovsky, and M. Rosenblum, *Phys. Rev. Lett.* **112**, 144103 (2014).
- ³⁵F. Böhm, A. Zakharova, E. Schöll, and K. Lüdge, *Phys. Rev. E* **91**, 040901 (R) (2015).
- ³⁶L. Schmidt and K. Krischer, *Phys. Rev. Lett.* **114**, 034101 (2015).
- ³⁷L. Schmidt and K. Krischer, *Chaos* **25**, 064401 (2015).
- ³⁸T. W. Ko and G. B. Ermentrout, *Phys. Rev. E* **78**, 016203 (2008).
- ³⁹A. Buscarino, M. Frasca, L. V. Gambuzza, and P. Hövel, *Phys. Rev. E* **91**, 022817 (2015).
- ⁴⁰C. R. Laing, *Phys. Rev. E* **81**, 066221 (2010).
- ⁴¹S. Loos, J. C. Claussen, E. Schöll, and A. Zakharova, *Phys. Rev. E* **93**, 012209 (2016).
- ⁴²V. Semenov, A. Zakharova, Y. Maistrenko, and E. Schöll, *EPL* **115**, 10005 (2016).
- ⁴³N. Semenova, A. Zakharova, V. Anishchenko, and E. Schöll, *Phys. Rev. Lett.* **117**, 014102 (2016).
- ⁴⁴N. C. Rattenborg, C. J. Amlaner, and S. L. Lima, *Neurosci. Biobehav. Rev.* **24**, 817 (2000).
- ⁴⁵N. C. Rattenborg, B. Voirin, S. M. Cruz, R. Tisdale, G. Dell'Omo, H. P. Lipp, M. Wikelski, and A. L. Vyssotski, *Nature Comm.* **7**, 12486 (2016).
- ⁴⁶C. R. Laing and C. C. Chow, *Neural Computation* **13**, 1473 (2001).
- ⁴⁷H. Sakaguchi, *Phys. Rev. E* **73**, 031907 (2006).
- ⁴⁸A. Rothkegel and K. Lehnertz, *New J. of Phys.* **16**, 055006 (2014).
- ⁴⁹A. E. Motter, S. A. Myers, M. Anghel, and T. Nishikawa, *Nature Phys.* **9**, 191 (2013).
- ⁵⁰J. C. Gonzalez-Avella, M. G. Cosenza, and M. S. Miguel, *Physica A* **399**, 24 (2014).
- ⁵¹O. E. Omel'chenko, *Nonlinearity* **26**, 2469 (2013).
- ⁵²J. Sieber, O. E. Omel'chenko, and M. Wolfrum, *Phys. Rev. Lett.* **112**, 054102 (2014).
- ⁵³C. Bick and E. A. Martens, *New J. Phys.* **17**, 033030 (2015).
- ⁵⁴I. Omelchenko, O. E. Omel'chenko, A. Zakharova, M. Wolfrum, and E. Schöll, *Phys. Rev. Lett.* **116**, 114101 (2016).
- ⁵⁵A. M. Hagerstrom, T. E. Murphy, R. Roy, P. Hövel, I. Omelchenko, and E. Schöll, *Nature Phys.* **8**, 658 (2012).
- ⁵⁶M. R. Tinsley, S. Nkomo, and K. Showalter, *Nature Phys.* **8**, 662 (2012).
- ⁵⁷S. Nkomo, M. R. Tinsley, and K. Showalter, *Phys. Rev. Lett.* **110**, 244102 (2013).
- ⁵⁸E. A. Martens, S. Thutupalli, A. Fourriere, and O. Hallatschek, *Proc. Natl. Acad. Sci. USA* **110**, 10563 (2013).
- ⁵⁹T. Kapitaniak, P. Kuzma, J. Wojewoda, K. Czolczynski, and Y. Maistrenko, *Sci. Rep.* **4**, 6379 (2014).
- ⁶⁰L. Larger, B. Penkovsky, and Y. Maistrenko, *Phys. Rev. Lett.* **111**, 054103 (2013).
- ⁶¹L. V. Gambuzza, A. Buscarino, S. Chessa, L. Fortuna, R. Meucci, and M. Frasca, *Phys. Rev. E* **90**, 032905 (2014).
- ⁶²L. Larger, B. Penkovsky, and Y. Maistrenko, *Nature Commun.* **6**, 7752 (2015).
- ⁶³M. Wickramasinghe and I. Z. Kiss, *PLoS ONE* **8**, e80586 (2013).
- ⁶⁴L. Schmidt, K. Schönleber, K. Krischer, and V. Garcia-Morales, *Chaos* **24**, 013102 (2014).
- ⁶⁵E. A. Viktorov, T. Habruseva, S. P. Hegarty, G. Huyet, and B. Kelleher, *Phys. Rev. Lett.* **112**, 224101 (2014).
- ⁶⁶V. Garcia-Morales and K. Krischer, *Contemporary Physics* **53**, 79 (2012).